Asian Journal of Physics
Vol. 33, No 12 (2024) 775-782
Available on: www.asianjournalofphysics.com

Shack-Hartmann null test using a pinhole array printed over a film screen

Javier Munoz-Lopez[a], Alberto Jaramillo-Nunez [a], Efren Santamaria-Juarez [b], Agustin Santiago-Alvarado and,[a,c] Alejandro Cornejo-Rodriguez[a]

[a]*Instituto Nacional de Astrofisica, Optica y Electronica* (*INAOE*)*, Optics Deparment, Luis Enrrique Erro 1, Puebla 72840, Mexico*

[b]*Instituto de Ciencias Aplicadas y Tecnologıa,* (*ICAT*) *Universidad Nacional Autonoma de Mexico* (*UNAM*),

Circuito Exterior S/N. Ciudad Universitaria, Coyoacan, 04510, Mexico City, Mexico

[c]*Universidad Tecnologica de la Mixteca (UTM), Carretera a Acatlima Km 2.5, Oaxaca 69000, Mexico*.

Dedicated to Prof (Dr) Daniel Malacara-Hernández

This work reports the calculation of the Shack-Hartmann null test and its experimental implementation through a pinhole array screen, printed over a Fluorinated Ethylene Propylene film, probing qualitatively a concave mirror using coherent and incoherent light sources.

doi: 10.54955.AJP.33.12.2024.775-782

Keywords: Ronchi test, Hartmann test, Shack-Hartmann test.

1 Introduction

The Ronchi test and the Hartmann test are used in the optical workshop to evaluate the final quality of optical surfaces under fabrication, both tests compare patterns from partial stages of the system against to an ideal reference pattern [1]. The reference pattern is numerically generated according to the design parameters. Currently, this task is also carried out using a Shack-Hartmann wavefront sensor (SHWs). The SHWs technique relies its operation principle on the Ronchi test and Hartmann tests, being part of the group known as screen tests.

In the SHWs test light comes from an optical system, passes through a micro lenslet array located close to the focus of the optical system or near to center of curvature of the surface under test, this allows to know the wavefront after a numerical processing. This feature results in SHWs being acknowledged as a testing method commonly used in the optical test laboratory and other areas of science and technology, such as astronomy [2] or ophthalmology [3]. On the other hand, the SHWs are expensive devices that require additional hardware, and their quality depends entirely on the quality of the micro lenslet array.

We propose an alternative method to know when the wavefront coming from a surface under fabrication has met the required design parameters. Based on the Ronchi test, and the Hartmann test, we applied the theory from the Hartmann null test [1,4], to compute the Shack-Hartmann null screen. The Shack-Hartmann null test avoids the construction of any other additional null optical system or null optical surface to probe the system under fabrication.

Corresponding author

e mail:jmunoz@inaoep.mx (Javier Munoz-Lopez)

The aim of the work is to obtain the Shack-Hartmann null spotfield, whose pattern is organized in a rectangular arrangement, easily recognizable by a technician in the workshop laboratory. The Shack-Hartmann null test avoids the construction of any other additional null optical system or null optical surface to probe the system under fabrication.

This work presents an innovation in the design and construction of the null screens, simplifying its fabrication. The null screen for the Shack-Hartmann test is generated using a pinholes array avoiding the micro lenslet array presented in the SHWs. The test is performed using coherent and incoherent lighting sources.

The paper is organised into five sections, including introduction. Section 2 includes a review on screen tests classic theory [1]. In section 3, the null Shack-Hartmann screen test is introduced, and the process to obtain the null screen is explained. Section 4 describes the experimental results. Finally, in section 5 conclusions and proposed future work are given.

2 Screen tests

The Ronchi, the Hartmann, and the Shack-Hartmann tests give information on the wavefront coming from the system being tested. All of them measure the wavefront slope giving us information on transverse aberration [1]. Using the Rayces formula [5] we represent them by

$$\frac{\partial W}{\partial x} = -\frac{TA_x}{l-W} - \frac{TA_x}{l};\ \frac{\partial W}{\partial y} = -\frac{TA_y}{l-W} - \frac{TA_y}{l}. \tag{1}$$

Here, W represents the wavefront, TA_x the transverse aberration along the x direction, TA_y the transverse aberration along the y direction, l measures the distance from the exit pupil of the system to the screen used in the Ronchi test along optical axis, L is the distance from the vertex to the center of curvature, d represents the distance between two consecutive dark fringes in the Ronchi ruling, see Fig (1),

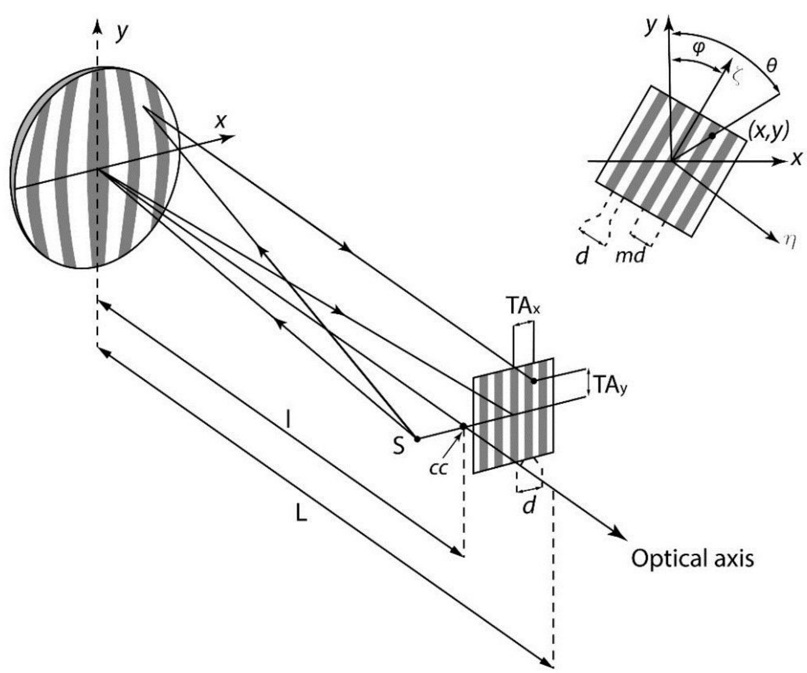

Fig 1. A screen test scheme, Ronchi test.

Cordero *et al* described Ronchi and the Hartmann tests on the same mathematical theory [6]. We apply that mathematical description to the Shack–Hartmann test, based on the similarity of their experimental setup and in the fact that the Hartmann test and the Shack-Hartmann test only differ where the plane of the screen grid is positioned [7].

According to Malacara [1] and Hopkins [8], the central point of each spot in a spotfield pattern in a Hartmann test, falls over lines following curves obtained in the Ronchi fringe pattern. Hence, we need to calculate the position for each spot in the null Shack-Hartmann spotfield pattern. We started from the transversal aberration expression, $TA(S)$ [9,10] as,

$$TA(S) = \frac{(l + L - 2z)\left[1 - \left(\frac{dz}{dS}\right)^2\right] + 2\frac{dz}{dS}\left[S - \frac{(l - z)(L - z)}{S}\right]}{\frac{l - z}{S}\left[1 - \left(\frac{dz}{dS}\right)^2\right] + 2\frac{dz}{dS}} \tag{2}$$

The variables involved in Eq (2) are schematized in Fig (2).

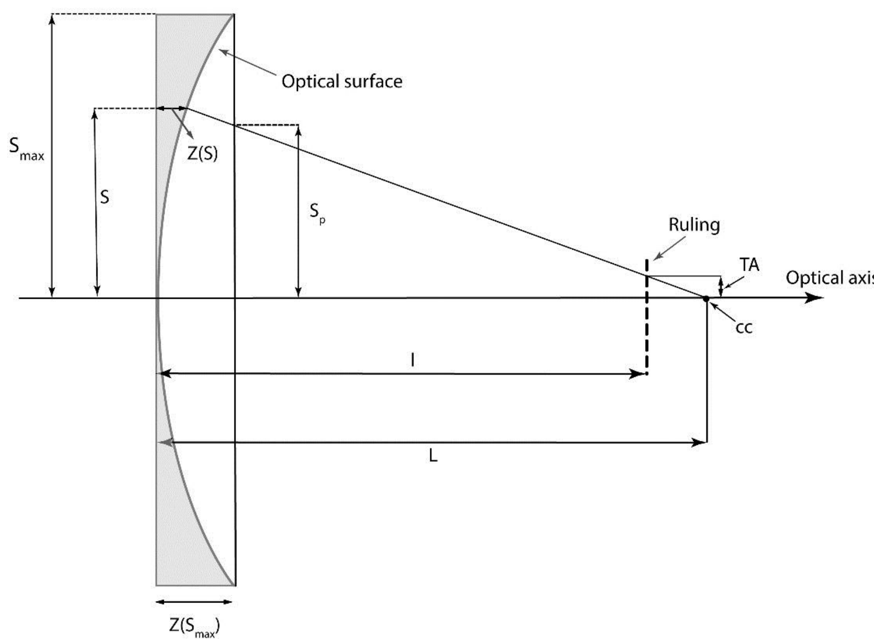

Fig 2. Variables used in transversal aberration $TA(S)$ expression.

Where S is a distance from the optical axis to a point over optical surface, Z is the sagitta function, φ represents the ruling inclination from the y-axis, and θ is the angle of any point (x,y) in the wavefront $W(x,y)$ over the Ronchi ruling.

Restricting this work to the case of $\varphi = 0$, we can express TA as:

$$TA(S) = \frac{md}{\sin\theta} \tag{3}$$

We evaluated the fringe pattern assigning values to S and calculating θ for different values of m, here md is the position along the η axis in the coordinate of the Ronchi ruling.

The error of considering the Ronchi fringes or the Hartmann screen over the surface instead of the exit pupil [1] is compensated through,

$$S_p = \left[1 - \left(\frac{z(S_{max}) - z(S)}{l - z(S)}\right)\left(1 - \frac{TA}{S}\right)\right] \tag{4}$$

here

$$z(S) = \frac{cS^2}{1 + \sqrt[2]{1 - (K+1)\,c^2S^2}} + A_1S^4 + A_2S^6 + A_3S^8 + A_4S^{10} \tag{5}$$

$S^2 = x^2 + y^2$, $c = 1/r$, and A_1, A_2, A_3, A_4 are the aspherical deformation constants, and K is the conic constant.

For all conical revolution surfaces, except paraboloid, we have.

$$z(S) = \frac{1}{K+1}\left[r - \sqrt[2]{r^2 - (K+1)S^2}\,\right] \tag{6}$$

The position of each pinhole in the Shack-Hartmann null screen [4,11], is given by

$$x = md,\ y = nd \tag{7}$$

Here, m and n are integer numbers, d represents the distance between two consecutive dark fringes, the transversal $TA(S)$ aberration represents the distance from any point to the origin of the coordinate system expressed by the Eq (2), that now takes the form,

$$TA(S) = d\left(\sqrt[2]{m^2 + n^2}\right) \tag{8}$$

through Eq (8) and Eq (2), we obtain a value for Eq (3). The position (x, y) of each spot center is given by

$$x_P = S_p\left(\frac{m}{\sqrt{m^2 + n^2}}\right);\ y_P = S_p\left(\frac{n}{\sqrt{m^2 + n^2}}\right) \tag{9}$$

We solve Eq (8) as a function of S. Equation (9) gives us the position of the entire spotfield pattern in the Shack-Hartmann null screen grid.

3 Null Shack-Hartmann screen fabrication

In a previous work, we reported the implementation of the Shack-Hartman test with a microholes grid screen [12]. That screen was developed using a microlithography process, showing the feasibility of replacing the lenslet array with a pinhole array. Now, as one of the main aims of this paper, we go a step forward, by simplifying the screen fabrication avoiding the microlithography process, shifting the procedure to a negative print process as described in the next paragraph.

The null Shack-Hartmann plate presented here represents a great simplification compared to any other kind of null test [13,14] or null optical configuration that requires additional optical elements, extra surfaces or compensators [15,16]. Making this null test easy access, fast made and reliable allowing it to be used in any optical workshop or optical test laboratory.

Once the calculation of the null pinhole geometric array distribution is done, as described in section two, the set of points is imported into vector graphics software; allowing us to draw apertures centered in the correspondent point position, the apertures could be modeled with different geometries such as circular apertures with 150 μm in diameter or square apertures with also 150 μm per side. After this digital treatment the screen is printed in a FEP (Fluorinated Ethylene Propylene) film sheet, through a commonly lithographic process used in offset printing. The printing process also has the capability of printing negative films at a resolution of 600 points per inch, giving us the ability of printing geometric apertures with 100 μm in size and a pitch of 300 μm, with a total contrast change from zero to one at a single point of resolution. The printing process is also cheaper and faster compared to the previous microlithography process.

It is essential to mention that the pinhole distribution in the Shack-Hartmann null screen requires to considers two cases depending on where the null screen will be located at the experimental setup, the first case will be positioned in a plane before the curvature center (BCC) the second case will be set in a plane after the curvature center (ACC). Figure (3) display examples of the pinhole distribution in the Shack-Hartman null screen for both cases BCC and ACC. Here we can see a distribution of white dots over a black background, this is shown not to scale and without any assigned dimension.

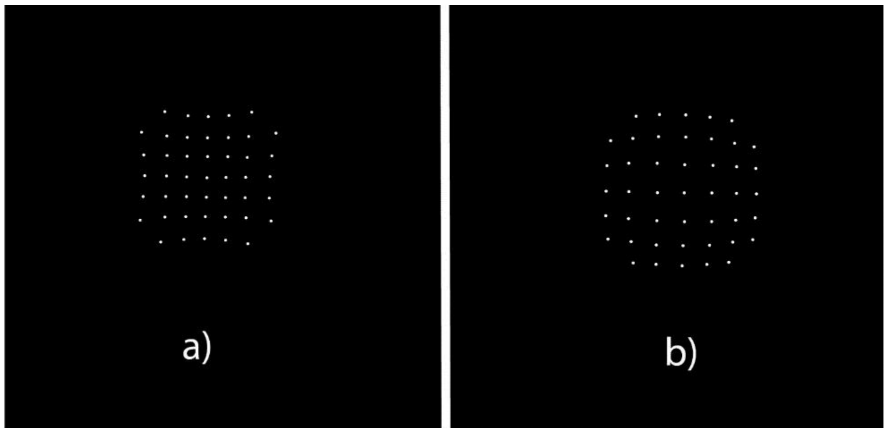

Fig 3. Pinhole distributions in Shack-Hartmann null grid screens: (a) used at BCC, and (b) used at ACC.

4 Experimental results

The experimental setup used in the Shack-Hartmann null test is schematized in Fig (4). Light beam from a point source PS is reflected from a concave parabolic surface producing a source image PS', PS & PS' are located outside the optical axis in the paraxial region at the same plane as the curvature center CC. The Shack-Hartman null screen is positioned perpendicular to the optical axis, at BCC plane or ACC plane, it must be located precisely in the calculated plane. The null Shack-Hartmann spotfield observed is registered in a posterior plane perpendicular to the optical axis, called NSH plane.

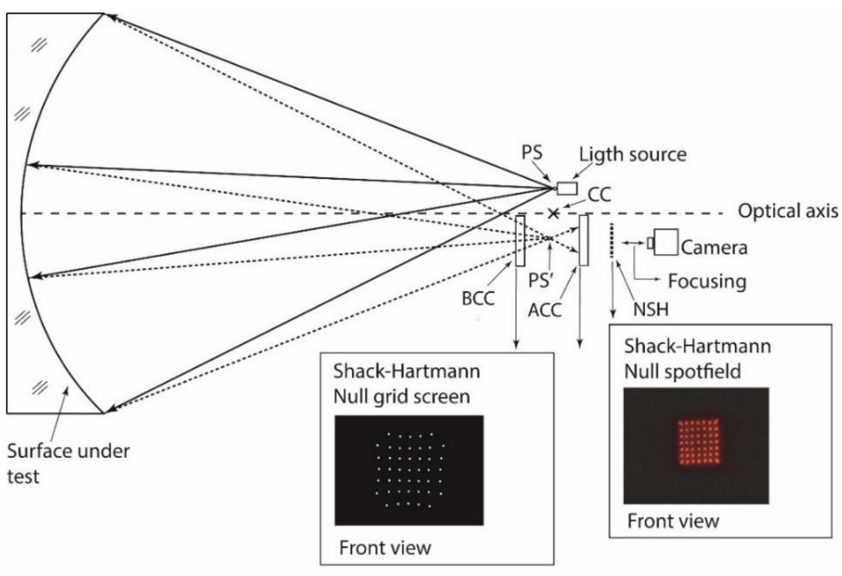

Fig 4. Shack-Hartmann null screen test experimental setup scheme.

When the surface under test meets the parameters established in the design stage, the optical element is considered well fabricated. Then, when applying the Shack-Hartmann null test, the spotfield pattern retrieved should be arranged in a rectangular uniform spotfield, This condition is easily recognizable by the technician who carried out the test.

We applied the Shack-Hartmann null test to a concave parabolic surface, which has a diameter of 110 mm and a radius of curvature of 950 mm and a conic constant $K = -1$.

In Fig (5) the Ronchi patterns and the Shack-Hartmann spotfield patterns obtained for the element under test are shown. The Ronchi patterns, as well as the Shack-Hartmann patterns, must be registered at the BCC and ACC planes, in our case at 10 mm from the point PS.

The Shack-Hartmann spotfield was recorded using a Shack-Hartmann plate with microholes of 100 µm in diameter and a pitch of 400 µm. Pictures in Fig (5) and all pictures displayed henceforth were registered with a CCD camera, calibrated to remove effects of lens distortion with an overall mean error of 2.2 pixels to record planar objects.

In Fig (5c) there is a distortion effect observable on some of the spots at the border of the vision field when we are close to the exit pupil of the element under test. This effect changes the fringe order as we change the plane position of the Shack-Hartmann plate, and it is more pronounced at the BCC planes, without affecting our results.

When testing the designed Shack-Hartmann null screen, three different LED light sources were used, one incoherent white light source, and two coherent light sources. The first coherent light source emitting at $\lambda = 632$nm and the second one emitting at $\lambda = 550$ nm. We performed the experiment with different light sources, since Ronchi test and the Shack-Hartmann test can be done with coherent and incoherent light sources.

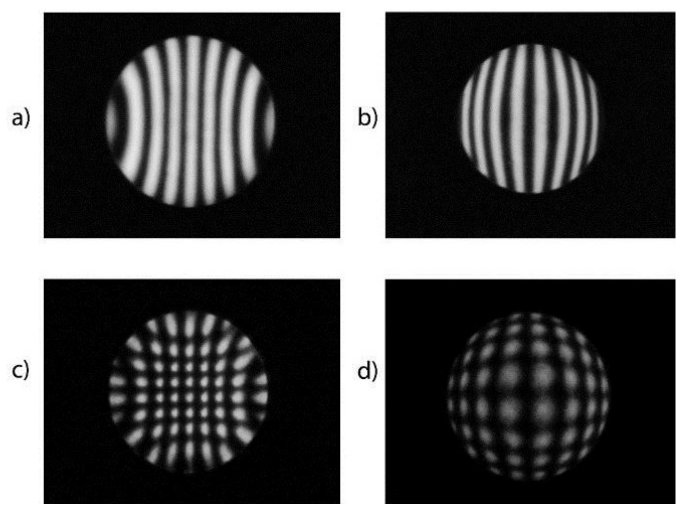

Fig 5. Ronchi patterns and Shack-Hartmann spotfield patterns at (a and c) BCC plane, (b and d) at ACC plane.

Figure (6) shows the spotfield patterns obtained for the different light sources configurations, as we proposed. We retrieve a set of spotfield patterns organized in a rectangular arrangement. Even though the null spotfield presents modulation due to diffraction effect and some spot deformation in the elements of the corner, the spotfield array stays in rectangular array.

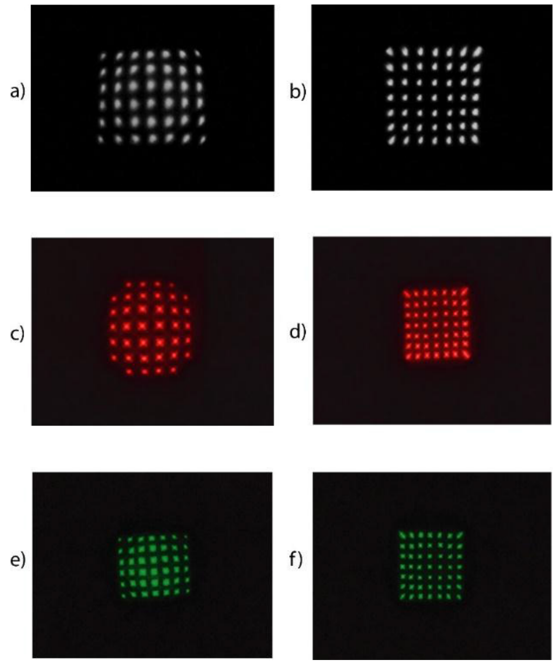

Fig 6. Shack-Hartmann null spotfield patterns, (a) at BCC plane, (b) at ACC plane both using an incoherent light source, (c) at BCC plane, (d) at ACC plane both using a coherent light source at λ = 632 nm. (e) at BCC plane, (f) at ACC plane both using a coherent light source at λ = 550 nm.

4 Conclusions

We succeeded in developing an accessible, convenient, and inexpensive method to get a qualitative Shack-Hartmann null test, using the same mathematical concepts as in the ideal Ronchi test and Hartmann test. This method is reachable and appropriate to be used by any optical surface test laboratory. The Shack-Hartmann null screen permits us to know when an optical surface under test meets the projected parameters required by its design, recovering a rectangular spotfield pattern easily recognizable. The observed pattern is a null test since the Shack-Hartmann null screen developed compensates the profile of the surface under test.

In a forthcoming paper, a polynomial wavefront representation will be presented to complement the qualitative analysis developed in this work.

Acknowledgements

Agustin Santiago Alvarado is grateful to CONAHCYT for the sabbatical scholarship with registry number I0200/111/2024.

References

1. Malacara D, Optical shop testing, Chapter 9. Wiley Series in Pure and Applied Optics, Wiley, 2007.
2. Malacara D, Malacara Z, Handbook of optical systems, CRC Press, Taylor and Francis Group, Boca Raton, FL, 2013.
3. Schwiegerling J, Field guide to visual and ophthalmic optics, (SPIE Press, Bellingham, WA), 2004.
4. Cordero A, Cornejo A, Cardona O, Null Hartmann and Ronchi-Hartmann tests, *Appl Opt*, 29(1990)4618–4621.

5. Rayces J L, Exact relation between wave aberration and ray aberration, *Opt Acta*, 11(1964)85–88.
6. Cordero A, Cornejo A, Cardona O, Ronchi and Hartmann Test with the same mathematical theory, *Appl Opt*, 31(1992)2370–2375.
7. Granados-Agustin F S, Cardona-Nunez O, Diaz-Uribe R, Percino-Zacarías E, Zárate-Rivera A M, Cornejo-Rodríguez A, Analysis of the common characteristics of the Hartmann, Ronchi, and Shack–Hartmann tests, *Optik*, 125(2014)667–670.
8. Hopkins G W, Shagam R N, Null Ronchi from spot diagrams, *Appl Opt*, 16(1977)2602–2603.
9. Sherwood A A, Ronchi test charts for parabolic mirrors, J Proc R Soc, New South Wales, 43(1960)19.
10. Malacara D, Geometrical Ronchi test of aspherical mirrors, *Appl Opt*, 4(1965)1371–1373.
11. Malacara D, Cornejo A, Null Ronchi test for a spherical surfaces, *Appl Opt*, 13(1974)1778–1780.
12. Nunez A J, Juarez E S, Muñoz-López J, Rodriguez A C, Testing concave optical surface by Shack-Hartmann test using microholes, *Opt Eng*, 61(2022)104104; doi: 10.1117/1.OE.61.10.104104.
13. Wang J, Wang X, Lirong Peng L, Wang J, Liu Z, Li L, Cai M, Liu B, Li W, Zhang X, Method for testing freeform surfaces based on a Shack-Hartmann sensor with plane wavefront scanning and stitching, *Opt Express*, 31(2023) 36702–36724.
14. Jalife-Chavira J M, Trujillo-Schiaffino G, Mendoza-Villegas P G, Salas-Peimbert D P, Anguiano-Morales M, Corral-Martínez L F, Tornero-Martínez N, Inverse Hartmann test for radius of curvature measurement in a corneal topography calibration sphere, *Rev Sci Instrum*, 93(2022)043101; doi:10.1063/5.0080572.
15. Aguirre-Aguirre D, Villalobos-Mendoza B, Díaz-Uribe R, Campos-García M, Null-screen design for highly freeform surface testing, *Opt Express*, 28(2020)36706–36722.
16. Muñoz-Potosi A F, Granados-Agustín F, Campos-García M, Valdivieso-González L G, Percino-Zacarias M E, Deflectometry using a Hartmann screen to measure tilt, decentering and focus errors in a spherical surface, *Opt Commun*, 402(2017)375–381.

[*Received*: 04.12.2024; *Rev recd*: 28.12.2024; *accepted*: 28.12.2024]

Javier Munoz-Lopez received his B Sc degree in physics from the BUAP in 1992, his M Sc degree in optics from the INAOE in 1995, and his PhD in optics also from INAOE in 1999. He currently holds a researcher position at INAOE, his subject interests include scattering and optical instrumentation.